Bioorganic & Medicinal Chemistry 19 (2011) 7526–7533

Contents lists available at SciVerse ScienceDirect

Bioorganic & Medicinal Chemistry

journal homepage: www.elsevier.com/locate/bmc

Disulfide and amide-bridged cyclic peptide analogues of the $VEGF_{81-91}$ fragment: Synthesis, conformational analysis and biological evaluation

María Isabel García-Aranda [a], Yasmina Mirassou [b], Benoit Gautier [c], Mercedes Martín-Martínez [a], Nicolas Inguimbert [c,†], Michel Vidal [c,‡], María Teresa García-López [a], María Angeles Jiménez [b], Rosario González-Muñiz [a], María Jesús Pérez de Vega [a,*]

[a] Instituto de Química Médica, IQM-CSIC. C/Juan de la Cierva, 3. 28006 Madrid, Spain
[b] Instituto de Química-Física Rocasolano, CSIC. C/Serrano, 119. 28006 Madrid, Spain
[c] Université Paris Descartes, UFR Biomédicale, Laboratoire de Pharmacochimie Moléculaire et Cellulaire, INSERM U648, 45 rue des Saints Pères, Paris F-75006, France

ARTICLE INFO

Article history:
Received 26 July 2011
Revised 11 October 2011
Accepted 12 October 2011
Available online 18 October 2011

Keywords:
VEGF
Peptides
Solid-phase synthesis
Protein–protein interactions
Angiogenesis

ABSTRACT

The design, synthesis, conformational studies and binding affinity for VEGFR-1 receptors of a collection of linear and cyclic peptide analogues of the β-hairpin fragment $VEGF_{81-91}$ are described. Cyclic 11-mer peptide derivatives were prepared from linear precursors with conveniently located Cys, Asp or Dap residues, by the formation of disulfide and amide bridges, using solid-phase synthesis. Molecular modelling studies indicated a tendency to be structured around the central β-turn of the $VEGF_{81-91}$ β-hairpin in most synthesized cyclic compounds. This structural behavior was confirmed by NMR conformational analysis. The NHCO cyclic derivative **7** showed significant affinity for VEGFR-1, slightly higher than the native linear fragment, thus supporting the design of mimics of this fragment as a valid approach to disrupt the VEGF/VEGFR-1 interaction.

1. Introduction

In the last few years, major progress has been made in targeting angiogenesis for human therapy, not only for the treatment of cancer but also for other diseases, such as diabetic retinopathy and rheumatoid arthritis.[1,2] Angiogenic growth factors promote the building of the vascular net that provide the oxygen supply necessary for tissue growth and survival. Tumor angiogenesis is a crucial step in cancer development, as tumors have to develop a neovascular supply to grow and metastasize.[3] The tumor microenvironment produces pro-angiogenic growth factors, such as the vascular endothelial growth factor (VEGF) that exerts its biological activity through the interaction with its specific receptors VEGFR-1 (Flt-1) and VEGFR-2 (KDR).[4,5]

Focused on one of the regions described as key for the interaction of VEGF with its receptors, the 81–91 fragment located in loop 3,[6–8] we have recently described the preparation of hydrocarbon-bridged cyclic peptides designed to mimic the biological role of this hot-spot in the VEGF–VEGFRs interaction.[9] These compounds showed affinity for the VEGFR-1 receptor, although they did not accurately adopt the desired β-hairpin conformation found for the $VEGF_{81-91}$ fragment within the native protein, slightly distorted at the turn because of the presence of an extra residue (Fig. 1). We have also reported NMR conformational studies on disulfide cyclic analogues of the fragment 69–80 of Vammin, a VEGF isolated from snake venom.[10] These peptides were able to adopt the β-hairpin conformation of the native fragment, which prompted us to use this type of bridge to prepare cyclic analogues of the corresponding fragment of VEGF. Moreover, there are numerous examples in the literature in which a disulfide bridge stabilizes β-hairpin structures.[11–15] However, amide-bridges are less common for this purpose,[16,17] apart from head-to-tail cyclic peptides,[18,19] although they are able to stabilize type I and II β-turns in bicyclic peptides.[20]

Having all this in mind, we proposed to explore the use of different bridges[9] to get better mimics of the $VEGF_{81-91}$ fragment. Particularly, disulfide (S–S) and amide (CO–NH and NH–CO) bonds were explored for covalently joining two side-chains of facing residues in the antiparallel strands of the β-hairpin (Fig. 2). Location of the bridge was determined by the previous results on the hydrocarbon-bridged analogues, for which the best activities were found

* Corresponding author. Tel.: +34 91 562 2900; fax: +34 91 564 4853.
E-mail address: pdevega@iqm.csic.es (M.J. Pérez de Vega).
† Present address: Université de Perpignan Via Domitia, Laboratoire de Chimie des Biomolécules et de l'Environnement, EA 4215, 52 Avenue P. Alduy, Perpignan F-66860, France.
‡ Present address: Université Paris Descartes, UFR des Sciences Pharmaceutiques et Biologiques, UMR CNRS 8638, 4 Avenue de l'Observatoire, Paris F-75270, France, and Laboratoire de Pharmacologie-Toxicologie, Service de Pharmacie, GH Cochin - Hôtel Dieu - Broca, AP-HP, Paris, France.

0968-0896/$ - see front matter © 2011 Elsevier Ltd. All rights reserved.
doi:10.1016/j.bmc.2011.10.032

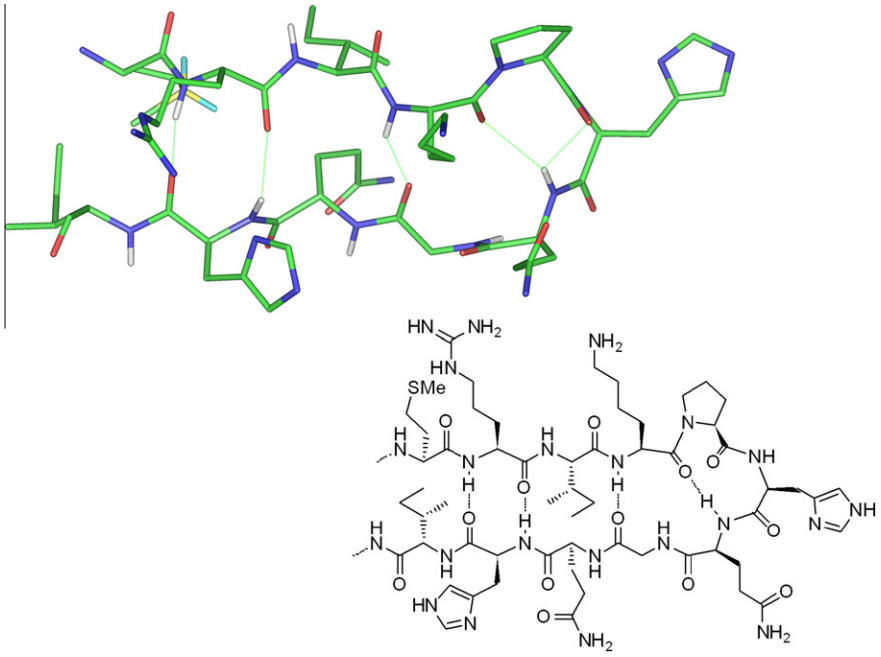

Figure 1. Three- and two-dimensional structure of the native VEGF–A_{81-91} fragment (from the crystal structure of VEGF–Flt1 complex, pdb code: 1flt).

81	82	83	84	85	86	87	88	89	90	91		
Ac-Met	**Arg**	**Ile**	**Lys**	**Pro**	**His**	**Gln**	**Gly**	**Gln**	**His**	**Ile-NH_2**	**1**	**(VEGF$_{81-91}$)**
Ac-Met	Cys	Ile	Lys	Pro	His	Gln	Gly	Gln	Cys	Ile-NH_2	**2**	
Ac-Met	Cys	Ile	Lys	Pro	His	Gln	Gly	Gln	Cys	Ile-NH_2	**3**	
					S—S							
Ac-Met	Asp	Ile	Lys	Pro	His	Gln	Gly	Gln	Dap	Ile-NH_2	**4**	
Ac-Met	Asp	Ile	Lys	Pro	His	Gln	Gly	Gln	Dap	Ile-NH_2	**5**	
					CO–NH							
Ac-Met	Dap	Ile	Lys	Pro	His	Gln	Gly	Gln	Asp	Ile-NH_2	**6**	
Ac-Met	Dap	Ile	Lys	Pro	His	Gln	Gly	Gln	Asp	Ile-NH_2	**7**	
					NH–CO							
Ac-Met	Asp	Ile	Lys	$^{\alpha Me}$Pro	His	Gln	Gly	Gln	Dap	Ile-NH_2	**8**	
Ac-Met	Asp	Ile	Lys	$^{\alpha Me}$Pro	His	Gln	Gly	Gln	Dap	Ile-NH_2	**9**	
					CO–NH							
Ac-Met	Dap	Ile	Lys	$^{\alpha Me}$Pro	His	Gln	Gly	Gln	Asp	Ile-NH_2	**10**	
Ac-Met	Dap	Ile	Lys	$^{\alpha Me}$Pro	His	Gln	Gly	Gln	Asp	Ile-NH_2	**11**	
					NH–CO							

Figure 2. Sequences of the designed VEGF$_{81-91}$ analogues.

for cycles formed through positions 2 and 10.[9] Therefore, the disulfide-bridged analogue **3** could be envisaged from the oxidation of the linear peptide derivative with Cys residues in positions 2 and 10 of the sequence. On the other hand, the amide-bridged cyclic analogues could be created by the appropriate introduction of Asp and Dap (α,β-diaminopropionic acid) residues, and further coupling of their side-chains. It should be taken into account that the CO and NH groups of the amide-bridge could participate in intramolecular hydrogen bonds, which could modify the global spatial structure. For this reason, the two possible bridges CO–NH (compound **5**) and NH–CO (compound **7**), containing Asp in position 2 and Dap in 10, or vice versa, were contemplated (Fig. 2). Additionally, replacement of the Pro residue by an α-Me-Pro to increase the conformational restriction was also considered (**9** and **11**). Moreover, the incorporation of an α,α-disubstituted amino acid, like α-MePro, would favor β-turn formation, which may also help the nucleation of the β-hairpin structure of the native protein.[21,22] Here we describe the synthesis, molecular modelling, NMR conformational analysis, and biological assays of these designed cyclic analogues (**3**, **5**, **7**, **9** and **11**) and their corresponding linear precursors (**4**, **6**, **8** and **10**; Fig. 2).

2. Results and discussion

2.1. Synthesis

The synthesis of the designed peptides was performed in parallel, following solid-phase synthesis protocols, using a Rink amide MBHA polystyrene resin and a Fmoc/tBu strategy. All compounds were isolated as amide at the C-terminal end, and acetylated at the N-terminal. To prevent aggregation problems and to favor intramolecular cyclization, a low load resin (0.34 mmol/g) was

used. Couplings to Pro and α-MePro residues were performed using 3 instead of 2 equiv of amino acids and reagents and repeating the coupling protocol three times to assure the complete reaction.

Preparation of the disulfide-bridged analogue **3** was accomplished from the linear derivative anchored to the resin by oxidation of Cys residues in positions 2 and 10. The use of an acetamidomethyl (Acm) protecting group for the –SH of Cys has allowed the selective deprotection of the sulfhydryl groups, as it is stable to mild acid and basic conditions.[23] Most of reagents described to remove the Acm group, such as Hg(II) salts/potassium ferricyanide, Tl salts, sulfenyl halides, and I_2, permit simultaneous deprotection and oxidation to the S–S bond, generating the disulfide-bridged cycle.[24–26] The desired compound **3** was obtained after several cyclization assays using different reagents and conditions (Table S1 of Supplementary data). In our case, the use of I_2 as oxidant under different conditions did not lead to the desired cyclic product, but to the linear dithiol derivative **2** (HPLC–MS). However, the cyclization was finally achieved by using $Tl(tfa)_3$ (thallium (III) trifluoroacetate) as reagent,[27,28] leading to the cyclic disulfide **3** in a high purity after semipreparative HPLC (Scheme 1).

The preparation of the amide-bridged cyclic analogues was performed by introduction of residues Asp and Dap in positions 2 and 10 of the sequence and subsequent coupling of their side-chains (Scheme 1). To perform the on-resin cyclization, an orthogonal protection strategy of the reactive groups of the side-chains of Asp and Dap residues was necessary. Thus, allyl esther and allyloxycarbonyl groups were used as Asp and Dap protectors to permit the selective deprotection of both groups with $PhSiH_3/Pd(PPh_3)_4$, without removal of the remaining side-chains protection until the final cleavage from the polymeric support. Lactamization to compound **5** was tried using a phosphonium or a uronium salt (PyAOP or HATU, respectively) as coupling reagent, which had proved to be particularly effective for couplings between side-chains.[29,30] The best results were obtained with PyAOP, leading to a higher percentage of the desired cyclic product **5** and a lower amount of the byproduct coming from the oxidation of the Met side-chain (HPLC–MS data, Table S2 of Supplementary data).

Lactamization to compound **5** was accomplished in 24 h, while only 2 h were necessary to obtain the NH–CO derivative **7**, using the same reaction conditions, which points to a preorganization of the linear peptide **6** that favor the cyclization. Analogues **9** and **11**, in which the Pro residue was replaced by α-MePro, were prepared under the same cyclization conditions used for the synthesis of **5** and **7** (Scheme 1). For both derivatives the lactam forming reaction was complete in a 2 h reaction time. Thus, the α-MePro could favor the formation of the β-turn ($VEGF_{84–87}$) that would approach the reactive groups and hence facilitate the intramolecular coupling.[31] Cyclic peptides **5**, **7**, **9** and **11** were isolated in satisfactory yields and high purity after semipreparative HPLC.

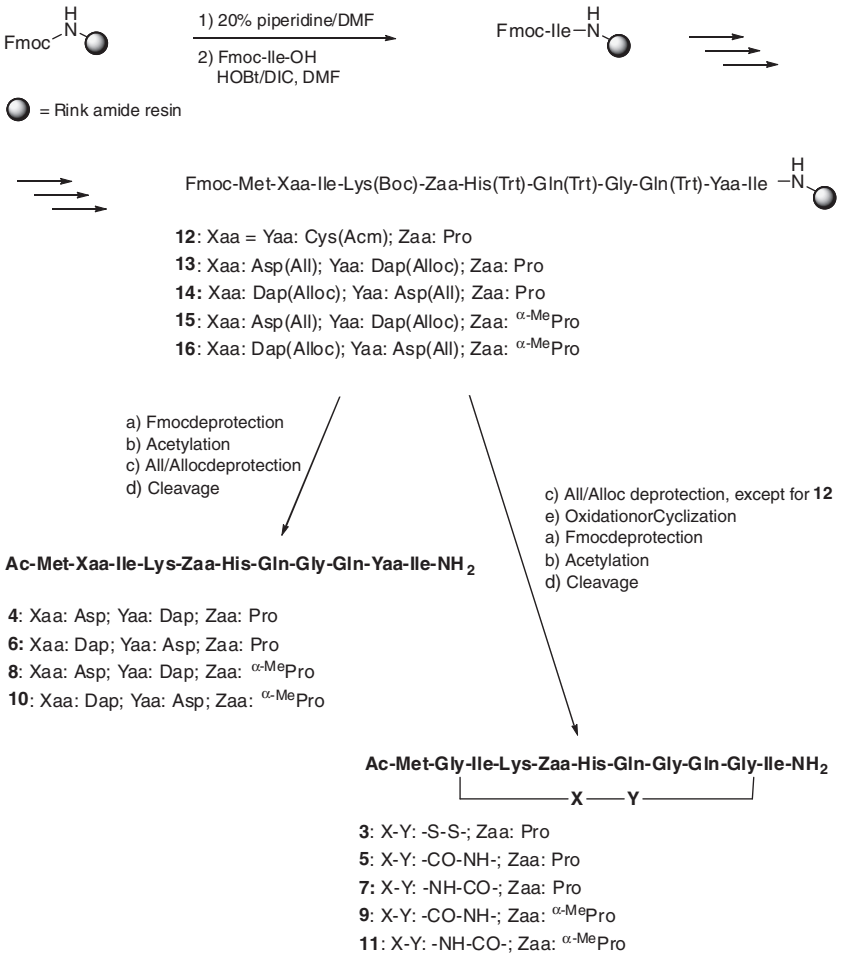

a) 20% Piperidine/DMF; b) Ac_2O, DMF, DIEA; c) $PhSiH_3$, $Pd(PPh_3)_4$, DCM, rt; d) TFA/EDT/H_2O/TIS (94:2.5:2.5:1), rt; e) Oxidation: Tl(tfa)3, DMF, rt; Cyclization: PyAOP, HOAt, DIEA, DMF, rt

Scheme 1. Synthesis of linear and cyclic peptides **3**–**11**.

2.2. Conformational analysis

2.2.1. Molecular modelling studies

The ability of the linear and cyclic derivatives to adopt conformations similar to the targeted β-hairpin, the structure of the native $VEGF_{81-91}$ fragment, was examined by simulated annealing molecular dynamics. For these studies the linear compound **4**, and the cyclic derivatives **5**, **7**, **9** and **11** were selected. The simulations were carried out using AMBER 10 suite of programs, and selecting different initial conformations for each peptide (see Section 4).

Theoretical calculations for linear derivative **4** indicated the existence of multiple conformations, in accordance with the flexibility showed by most linear peptides. Cyclic derivatives were also highly flexible, but they display a tendency to stabilize the central β-turn of the β-hairpin. The introduction of an α-MePro residue in **9** promotes the stabilization of this turn in a 72% of the conformers compared to the non-existence of this type of conformation in compound **5**. These data are in good agreement with the NMR results (see below), which indicated the lack of hydrogen bonds stabilizing the structure in compounds **4** and **5** (with a Pro5 residue), while the protection of the Gln7 NH was observed for peptides **8** and **9**, with an α-MePro residue. Molecular modelling data for this latter compound showed that the H-bond between this NH and the CO group of Lys4 is present in 63% of the conformers.

Concerning compounds with the NH–CO bridge, about 69% of the minimum energy conformers of Pro derivative **7** adopted the three first dihedral angles of the turn ($VEGF_{84-87}$ β-turn). However, in the case of the α-MePro analogue **11**, only 26 % of the conformers prove to have the Gln7 NH forming a H-bond with the Lys4 CO. Therefore, the presence of the α-MePro residue does not seem to favor the desired structure in this case. In fact, 21% of the conformers showed a H-bond between the NH of the bridge and the Met1 residue (Figs. S2 and S3 in Supplementary data).

2.2.2. NMR conformational analysis

The structural behavior of the cyclic and linear derivatives in solution was experimentally investigated by NMR spectroscopy. Derivatives **3**–**7** showed the two sets of NMR signals expected for Pro-containing peptides, corresponding to the *trans* and *cis*-Pro rotamers. The major species were confirmed to be the *trans*-Pro isomers by the presence of NOE cross-peaks between the Lys H_α proton and the Pro $H_{\delta\delta'}$ protons in the NOESY spectra, and by the differences between Pro $^{13}C_\beta$ and $^{13}C\gamma$ chemical shifts.[32] The presence of the *cis*-Pro isomers complicated spectral analysis in the case of the cyclic derivatives **3**, **5** and **7** that exhibit large percentages of the *cis*-Pro species (20–35% vs the 5–6% observed for the linear compounds **4** and **6**). No minor species were found for compounds **8–11** since α-MePro residues exist only as *trans* rotamers.[33] The analysis of NMR parameters refers from hereon to the major *trans*-Pro rotamer.

The strongest NMR evidence about the formation of ordered structures in peptides comes from the presence of non-sequential NOE cross-peaks. None of the NOEs involving backbone protons that are characteristic of the target β-hairpin (Figures in Table 1) were detectable in the NOESY spectra of these peptides. This indicated that neither the linear nor the cyclic derivatives adopt a native-like β-hairpin. This conclusion was further confirmed by the profiles of $^1H_\alpha$, $^{13}C_\alpha$ and $^{13}C_\beta$ conformational shifts ($\Delta\delta = \delta^{observed} - \delta^{random\ coil}$, ppm), which did not conform to that characteristic of β-hairpins.[34] In fact, the $^1H_\alpha$, $^{13}C_\alpha$ and $^{13}C_\beta$ conformational shifts, which are indicative of secondary structure because of their dependence on φ and ψ dihedral angles, displayed by peptides **3**–**11** (Fig. S1 in Supplementary data) were small in absolute value ($|\Delta\delta^{H\alpha}| < 0.1$ ppm, $|\Delta\delta^{C\alpha}| < 0.5$ ppm and $|\Delta\delta^{C\beta}| < 0.5$ ppm), particularly in the case of linear peptides, except for Lys4, which showed the characteristic behavior of Pro-preceding residues,[35] and for His6. However, some weak non-sequential NOEs were observed for all the cyclic peptides, except for peptide **3** (disulfide-bridge), and for the linear peptides **4** and **8.** These NOEs can be classified into two groups: (i) those involving Ile3 and Pro/αMePro5, and Lys4 and Gln7, and (ii) those between the bridge protons ($C_\beta H$ protons of residues 2 and 10) and either Pro/αMePro5 (in peptides **7** and **11**; NHCO-bridges) or the Lys4 side chain (in peptides **5** and **9**; CONH bridges). The first group of NOEs that is present in peptides **4**, **5**, **8**, **9** and **11** suggest some ordering at the turn region, as pointed out by the molecular modelling simulations for the cyclic peptides, and confirmed by the hydrogen-bonding analysis deduced from amide temperature coefficients (see below) for peptides **8**, **9** and **11** (Table 1). Regarding the second group of non-sequential NOEs, those involving bridge and turn protons, they are indicative of the bridge becoming closer to the backbone plane, and thus suggestive of a flattening of the structure. Likely, this flattened structure is more populated in peptide **11**, for which the bridge amide proton is solvent protected (see below). In brief, NOE and chemical shift data indicate that these peptides behave mainly as random coil in aqueous solution, but some ordering exists at the turn region, in particular in the cyclic analogues.

To ascertain whether in these analogues there are NH groups involved in the formation of hydrogen bonds, we determined the temperature coefficients ($\Delta\delta/\Delta T$) of amide protons of peptides **3**–**11** (Table 1). In aqueous solutions, temperature coefficients equal or less than 4 ppb/K (in absolute value) are indicative of a solvent-shielded NH proton,[36] which, in short peptides, is usually a consequence of the NH involvement in an intramolecular hydrogen bond. On the other hand, values over 5 ppb/K are suggestive of solvent accessibility, whereas those in the interval 4–5 ppb/K are not conclusive by themselves. According to this criteria all the amide protons (see the temperature coefficients at Table 1) were solvent accessible in the linear compounds **4** and **6**, and in the cyclic analogues **3** (S–S) and **5** (NH–CO). In contrast, the temperature coefficients observed for the linear α-MePro analogues **8** and **10**, and the cyclic derivatives **7**, **9** and **11** indicated that the NH of Gln7 was solvent-protected, and hence likely participating in an intramolecular hydrogen-bond. This Gln7 NH proton forms a hydrogen bond with the CO oxygen of Lys4 residue in the β-turn of the native VEGF structure (see top Figures in Table 1). Compound **11** showed the values of temperature coefficients slightly different from those of the rest of derivatives. In this case, the NH of the bridge was solvent-protected, while amide NHs of Lys4, Gly8 and Asp10 residues were in the uncertainty region (Table 1). This data points out to a more structured conformation for this analogue. In fact, this compound showed some more non-sequential NOE cross-peaks (see above).

In short, according to the NMR parameters, peptides **3**–**11** do not adopt the targeted β-hairpin structure, but they show some tendency to adopt the $VEGF_{81-91}$ β-turn structure, particularly the cyclic Pro analogue **7**, as well as the linear and cyclic α-MePro derivatives **8**–**11**.

2.3. Binding affinity for VEGFR-1

Synthesized peptides were evaluated for their ability to displace biotinylated $VEGF_{165}$, in a chemiluminescent assay relying on competition between tested compounds and biotinylated $VEGF_{165}$ for binding to the extracellular domain of recombinant VEGFR-1 (Table 2).[37,38]

The biological evaluation showed that most of the prepared compounds have certain affinity for the VEGFR-1 receptor. Low inhibition values were found for disulfide cyclic peptide **3**, as well as for amide CO–NH cycle **5**, that have no protected NHs from the solvent and, therefore, are highly flexible. By contrast cyclic

Table 1
Temperature coefficients for amide protons of the amide-bridged derivatives and their linear precursors

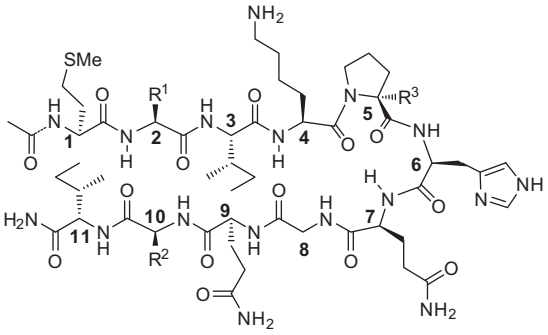

Linear compounds **4, 6, 8, 10**

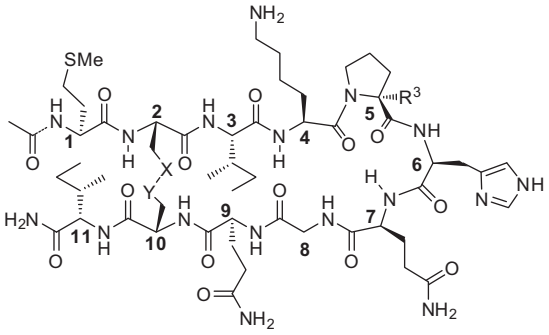

Cyclic compounds **5, 7, 9, 11**

Entry	R^1	R^2	R^3	X–Y	Δδ/ΔT (ppb/K)[a]										
					Met1	Position 2	Bridge NH	Ile3	Lys4	His6	Gln7	Gly8	Gln9	Position 10	Bridge NH	Ile11
3	—	—	H	S–S	−8.5	−6.5	—	−4.5	−6.8	−7.5	−6.5	−7.0	−6.5	−6.0[b]	—	−8.5
4	CH_2CO_2H	CH_2NH_2	H	—	−7.8	−6.1	—	−7.6	−9.1	−8.5	−8.2	−8.4	−6.8	ND	—	−8.9
5	—	—	H	CONH	−7.7	−5.7	—	−7.1	−6.8	−7.6	−5.3	−6.3	−6.8	−5.4	−5.7	−7.8
6	CH_2NH_2	CH_2CO_2H	H	—	−7.7	ND[b]	—	−9.2	−9.9	−8.7	−7.6	−7.8	−6.4	ND	—	−8.8
7	—	—	H	NHCO	−8.3	−6.5	−4.5	−5.8	−6.8	−5.8	−2.6	−7.4	−7.9	−5.9	—	−8.8
8	CH_2CO_2H	CH_2NH_2	Me	—	−7.7	−6.0	—	−7.4	−8.5	−7.6	−3.8	−7.6	−6.4	−6.5	—	−9.0
9	—	—	Me	CONH	−7.7	−5.9	—	−6.9	−6.7	−6.4	−3.7	−5.1	−6.9	−5.0	−4.5	−8.5
10	CH_2NH_2	CH_2CO_2H	Me	—	−7.8	ND	—	−9.1	−9.1	−5.9	−3.6	−6.9	−6.1	−6.2	—	−8.7
11	—	—	Me	NHCO	−7.8	−5.6	−0.9	−7.6	−4.5	−6.2	−1.4	−4.0	-9.7	−4.8	—	−9.1

[a] Calculated from NH chemical shifts measured in an aqueous solution H_2O/D_2O (9:1) at 5 °C and at 25 °C.
[b] ND = Non determined.

Table 2
Inhibitory potency of peptides **1**, **3**–**11** on VEGFR-1. Displacement assays.

Entry	Sequence	% Inhibition[a]	IC_{50}[b] (μM)	
		ECD	ECD	D1-D3
1	H-MRIKPHQGQHI-OH	45.1 ± 2.6	102.7 ± 5.3	160.0 ± 10.7
3	Ac-M-c(CH_2-S-S-CH_2)^{2,10} [GIKPHQGQG]I-NH_2	11.2 ± 2.1	—	—
4	Ac-MDIKPHQGQDapI-NH_2	24.6 ± 4.1	—	—
5	Ac-M-c(CH_2-CO-NH-CH_2)^{2,10} [GIKPHQGQG]I-NH_2	15.8 ± 3.2	—	—
6	Ac-MDapIKPHQGQDI-NH_2	25.3 ± 2.8	—	—
7	Ac-M-c(CH_2-NH-CO-CH_2)^{2,10} [GIKPHQGQG]I-NH_2	53.0 ± 2.2	93.2 ± 7	87.6 ± 5
8	Ac-MDIK$^{\alpha\text{-Me}}$PHQGQDapI-NH_2-NH_2	11.4 ± 2.3	—	—
9	Ac-M-c(CH_2-CO-NH-CH_2)^{2,10} [GIK$^{\alpha\text{-Me}}$PHQGQG]I-NH_2	38.0 ± 2.5	—	—
10	Ac-MDapIK$^{\alpha\text{-Me}}$PHQGQDI-NH_2	3.1 ± 2.6	—	—
11	Ac-M-c(CH_2-NH-CO-CH_2)^{2,10} [GIK$^{\alpha\text{-Me}}$PHQGQG]I-NH_2	2.8 ± 2.9	—	—

[a] Activity corresponds to the percentage of biotinylated $VEGF_{165}$ displaced by a concentration of peptide of 100 μM on the whole extracellular domain (ECD) of VEGFR-11 (±SEM).
[b] Concentration of compound able to displace 50% the binding of biotinylated VEFG165 on VEGFR-1 either on the whole extracellular domain (ECD), or at the D1–D3 domains (±SEM).

analogue **7** with the NH–CO bridge, which proved to have certain structure around the β-turn, displayed a much better affinity value than its linear unstructured precursor. Concerning compounds in which the Pro residue was replaced by α-MePro, cyclic peptide **9**, with a CO–NH bridge, showed also better percentage of biotinylated $VEGF_{165}$ displacement than its linear precursor **8**, in accordance with the higher degree of structure pointed out by modelling and corroborated by NMR data. For the pair formed by the linear compound **10** and its corresponding amide NH–CO bridged peptide, **11**, they proved to be unable to inhibit the VEGF–VEGFR-1 interaction. This could be explained by the adoption of substantially different conformations with respect to the native structure (Fig. S3 in Supplementary data). In general, it seems that the affinity of these compounds for the VEGFR-1 receptor is related to their ability to stabilize a β-turn in the fragment spanning 84–87 residues.

Compound **7**, showing a 53% inhibition, was selected for dose–response studies, and was tested both on the whole extracellular domain of the receptor (D1–D7) and on the D1–D3 immunoglobulin domains of VEGFR-1, the specific domains for VEGF binding (Table 2, Fig. 3). The IC_{50} values observed were very similar in both assays (93.2 ± 7 μM and 87.6 ± 5 μM, respectively), therefore, it can be suggested that the interaction of compound **7** with the receptor takes place through the same region than with the native ligand, VEGF. Compared with the previously prepared hydrocarbon-bridged cyclic compounds,[9] the percentages of inhibition found for these new analogues were of the same order. However, in this case the more flexible linear analogues did not showed any significant affinity values, while in the case of the formerly reported hydrocarbon-bridged derivatives their bis-allylGly linear precursors showed better affinities than the corresponding restricted cyclic peptides. It could be

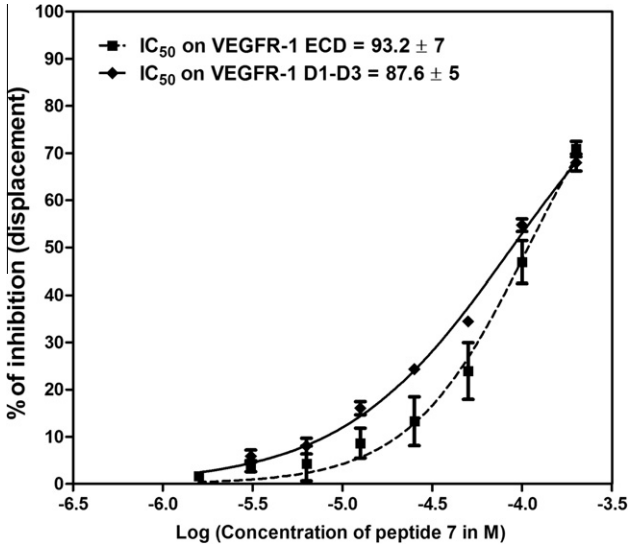

Figure 3. Effect of peptide **7** on VEGFR-1 displacement assays (VEGFR-1 ECD in continuous line and VEGFR-1 D1–D3 in dashed line).

assumed that substitution of Arg and His residues is responsible of the low affinity values found for the Asp/Dap derivatives described herein, when compared to the parent compound **1**. However, in our previous work with the hydrocarbon-bridged analogues, the 2,10-bis(allylGly) substituted linear precursors proved to be active, showing even higher affinity for the VEGFR-1 than the corresponding cyclic analogues.[9] This states the relative low importance of basic residues Arg2 and His10 in the VEGF–VEGFR-1 interaction, but the incorporation of a residue of a very different character, as the acidic Asp, seems to be detrimental for receptor recognition. Comparing the different nature of the bridges in cyclic derivatives in general it can be said that hydrocarbon bridges led to better affinity results than disulfide and amide bridges.

Worth to mention are the results found for cyclic peptide **7** (NH–CO bridge) that surpassed the affinity of the native linear $VEGF_{81-91}$ fragment, and is the analogue having the highest percentage of conformers with β-turn structure (as indicated by the modelling studies and in accordance with the results of RMN experiments).

3. Conclusions

In summary, a small collection of linear and cyclic analogues of $VEGF_{81-91}$ fragment has been synthesized. Some of these compounds proved to interact with the VEGFR-1 receptor, with the best results found for the cyclic NH-CO amide-bridged Pro derivative **7**. Conformational studies indicated that cyclic amide-bridged peptides, had a certain tendency to be structured around the central β-turn of the $VEGF_{81-91}$ β-hairpin, but the whole native structure could not be accurately stabilized. However, this tendency seems to be related to their ability to bind to VEGFR-1 receptors, at least for cyclic compounds. The results found in the binding experiments for compound **7** encourage us to further investigate the length, position and nature of the bridge, with the aim of stabilizing the β-hairpin structure of the native fragment, and attempting to better disrupt the VEGF–VEGFR-1 interaction.

4. Experimental section

4.1. Synthesis of linear and disulfide- and amide-bridged cyclic derivatives 3–11. General procedure

Resin bound peptides were synthesized by conventional Fmoc solid-phase chemistry[39–41] on a MBHA-Rink amide resin.[42] In each coupling step, the appropriate Fmoc amino acid (1.5 equiv) was treated with HOBt/DIC (1.5 equiv) in anhydrous DMF or with HCTU/DIEA (2 equiv). Couplings were allowed to proceed at room temperature overnight or for 1 h, respectively. The coupling efficiency was monitored by ninhydrin or chloranil test, and when necessary repeated with a fresh portion of Fmoc-amino acid and the indicated coupling reagents. After each coupling step, the Fmoc group was removed by treatment with 20% piperidine in DMF (3 × 10 min). For disulfide bridge formation, a solution of $Tl(tfa)_3$ (22 mg, 0.408 mmol) in DMF (2 ml) was added to resin-bounded derivative (100 mg, 0.034 mmol). The reaction mixture was stirred for 90 min. The resin was washed and drained with DMF/DCM/DMF/DCM (4 × 0.5 min). For amide bridge formation, after removing of Alloc and OAll protecting groups, the linear-resin-bounded derivative (100 mg, 0.034 mmol), was treated with a solution of PyAOP (177 mg, 0.34 mmol), HOAt (46 mg, 0.34 mmol), DIEA (0.12 ml, 0.68 mmol) in anhydrous DMF (2 ml). The reaction was allowed to proceed at room temperature until ninhydrin test was negative. The resin was washed and drained with DMF/DCM/DMF/DCM (4 × 0.5 min). After Fmoc deprotection and before cleavage from the resin, all derivatives were acetylated by treatment with a mixture of Ac_2O/DIEA in DMF (4 × 10 min) and then washed with DMF and DCM. Finally, the resin was treated with the cleavage cocktail TFA/EDT/H_2O/TIS (94:2.5:2.5:1) for 5 h at room temperature. The filtrates were precipitated from diethylether, centrifuged and lyophilized, and the resulting mixture was purified by reverse phase semipreparative HPLC to obtain the peptides 3–11 in 6–29% overall yield (calculated on the bases of resin substitution). See Supplementary data for details.

4.2. Molecular modelling studies

All Simulations and calculations were carried out with the AMBER 10 suite of programs,[43–45] using AMBER ff99 force field, and generalized Amber force field (GAFF) to generate parameters for the bridges. Peptides were initially built in extended conformations. The generalized Born/surface area (GB/SA) implicit solvent model (igb = 1) was used to model the effects of solvatation. An integration step of 1.0 fs and a 24 Å nonbonded cutoff were applied. Unless otherwise indicate, the SHAKE algorithm was used. Each structure was subjected initially to 5000 steps of steepest descent minimization and 5000 steps of conjugate gradient, followed by an equilibration of 40 ps where the temperature was established at 300 K. Then, the resulting structure was slowly heated to 1000 K increasing the temperature up to 600, 800 and 1000 K, each during 50 ps, and allowing and equilibration of 50 ps at each temperature, and an extra 50 ps at 1000 K. Subsequently the system was cooled slowly to 300 K in steps. In each step the temperature was lowered by 100 K (50 ps), and was kept at this temperature during 50 ps. After cooling at 300 K, a molecular dynamic simulation was carried out at this temperature for 200 ps, without the SHAKE algorithm. The conformer obtained is stored and used to start a new simulation at high temperature. Each conformer is energy-refined using 5000 steps of steepest descent minimization and 5000 steps of conjugate gradient. This procedure samples 100 energy-minimized conformations.

4.3. 2D NMR spectroscopy

Samples were prepared by dissolving the lyophilized peptide (~1 mg) in H_2O/D_2O (9:1 in volume; 0.5 mL) or in pure D_2O (0.5 mL). Peptide concentrations were about 1–2 mM. pH was adjusted to 5.5 by adding minimal amounts of NaOD or DCl, measured with a glass micro electrode and not corrected for isotope effects. The temperature of the NMR probe was calibrated using

a methanol sample. Sodium 2,2-dimethyl-2-silapentane-5-sulfonate (DSS) was used as an internal reference. NMR spectra were acquired at 5 °C in a Bruker Avance-600 spectrometer operating at a proton frequency of 600.13 MHz and equipped with a cryoprobe. 1D ^{1}H NMR spectra were acquired using 32 K data points, which were zero-filled to 64 K data points before performing the Fourier transformation. As previously reported,[46] phase-sensitive two-dimensional correlated spectroscopy (COSY), total correlated spectroscopy (TOCSY), and nuclear Overhauser enhancement spectroscopy (NOESY) spectra were recorded by standard techniques using presaturation of the water signal and the time-proportional phase incrementation mode. NOESY mixing times were 150 ms and TOCSY spectra were acquired using 60 ms DIPSI2 with *z* filter spin-lock sequence. The $^{1}H–^{13}C$ heteronuclear single quantum coherence spectra (HSQC) at natural ^{13}C abundance were recorded in 1–2 mM peptide samples in D_2O. Acquisition data matrices were defined by 2018 × 512 points in t_2 and t_1, respectively. Data were processed using the standard TOPSPIN program.[47] The 2D data matrix was multiplied by either a square-sine-bell or a sine-bell window function with the corresponding shift optimized for every spectrum and zero-filled to a 2 K × 1 K complex matrix prior to Fourier transformation. Baseline correction was applied in both dimensions. The 0 ppm ^{13}C δ-value was obtained indirectly by multiplying the spectrometer frequency that corresponds to 0 ppm in the ^{1}H spectrum, assigned to internal DSS reference, by 0.25144953.[48] Standard sequential assignment methods[43,49,50] were applied to assign the ^{1}H NMR signals of the peptides. Then, the ^{13}C resonances were straightforwardly assigned based on the cross-correlations observed in the HSQC spectra between the proton and the bound carbon. Additional 2D TOCSY spectra were recorded at 25 °C to examine the temperature dependence of amide proton chemical shifts.

4.4. Chemiluminescent competition assays

The surface of white high-binding 96-well microplate was coated with 100 μl of phosphate-buffered saline solution (PBS, pH 7.4) containing either VEGFR-1 ECD/Fc Chimera (20 ng/well) or VEGFR-1 D1–D3/Fc chimera (15 ng/well) and incubated at 4 °C overnight. After three washes with 250 μl of PBS 0.1%, (v/v) Tween 20 (buffer A), the plate was blocked by 200 μl of PBS with 3% (w/v) of BSA and stirred at 37 °C for 2 h. The plate was washed three times with buffer A. Then, 100 μl of a solution containing 131 pM of $btVEGF_{165}$ and the tested compounds at various concentration diluted in PBS containing 1% DMSO were added in each well. After 3 h stirring at 37 °C, the plate was washed four times with buffer A and 100 μl of streptavidin-horseradish peroxidase diluted at 1:8000 in PBS containing 0.1% (v/v) Tween 20 and 0.3% (w/v) BSA were added per well. After 1 h of incubation at 37 °C under obscurity and stirring, the plate was washed five times with 250 μl of buffer A and 100 μl of the chemiluminescent substrate were added. The remaining bt-$VEGF_{165}$ was detected by chemiluminescence, which was quantified. The percentages of $btVEGF_{165}$ displacement were calculated by the following formula: percentage of displacement = $100 * [1 - (S - NS)/(MS - NS)]$, where S is the signal measured, NS is the nonspecific binding signal and MS is the maximum binding signal observed with $btVEGF_{165}$ without compounds tested.

Acknowledgments

This work was supported by the Spanish Ministry of Science and Innovation (SAF 2006-01205, SAF 2009-09323 & CTQ2008-0080/BQU), and the CSIC (PIF 2005-80F0161, PIF 2005-80F0162 and PIE 2006-80I066). M.I.G.-A. and Y.M. thank the CSIC for predoctoral fellowships, and M.I.G.-A. thanks the SEQT (Spanish Society of Therapeutic Chemistry) for the Ramón Madroñero Award (XIV edition, 2009).

Supplementary data

Supplementary data associated with this article can be found, in the online version, at doi:10.1016/j.bmc.2011.10.032.

References and notes

1. Ferrara, N.; Kerbel, R. S. *Nature* **2005**, *438*, 967.
2. Carmeliet, P. *Nat. Med.* **2003**, *9*, 653.
3. Feron, O. *Trends Pharmacol. Sci.* **2004**, *25*, 536.
4. Gille, H.; Kowalski, J.; Li, B.; LeCouter, J.; Moffat, B.; Zioncheck, T. F.; Pelletier, N.; Ferrara, N. *J. Biol. Chem.* **2001**, *276*, 3222.
5. Kanno, S.; Oda, N.; Abe, M.; Terai, Y.; Ito, M.; Shitara, K.; Tabayashi, K.; Shibuya, M.; Sato, Y. *Oncogene* **2000**, *19*, 2138.
6. Keyt, B. A.; Nguyen, H. V.; Berleau, L. T.; Duarte, C. M.; Park, J.; Chen, H.; Ferrara, N. *J. Biol. Chem.* **1996**, *271*, 5638.
7. Muller, Y. A.; Christinger, H. W.; Keyt, B. A.; de Vos, A. M. *Structure* **1997**, *5*, 1325.
8. Muller, Y. A.; Li, B.; Christinger, H. W.; Wells, J. A.; Cunningham, B. C.; de Vos, A. M. *Prod. Natl. Acad. Sci. U.S.A.* **1997**, *94*, 7192.
9. García-Aranda, M. I.; Marrero, P.; Gautier, B.; Martín-Martínez, M.; Inguimbert, N.; Vidal, M.; García-López, M. T.; Jiménez, M. A.; González-Muñiz, R.; Pérez de Vega, M. J. *Bioorg. Med. Chem.* **2011**, *19*, 1978.
10. Mirassou, Y.; Santiveri, C. M.; Perez de Vega, M. J.; Gonzalez-Muniz, R.; Jimenez, M. A. *ChemBioChem* **2009**, *10*, 902.
11. Karle, I. L.; Kishore, R.; Raghothama, S.; Balaram, P. *J. Am. Chem. Soc.* **1988**, *110*, 1958.
12. McDonnell, J. M.; Fushman, D.; Cahill, S. M.; Sutton, B. J.; Cowburn, D. *J. Am. Chem. Soc.* **1997**, *119*, 5321.
13. Syud, F. A.; Espinosa, J. F.; Gellman, S. H. *J. Am. Chem. Soc.* **1999**, *121*, 11577.
14. Cochran, A. G.; Tong, R. T.; Starovasnik, M. A.; Park, E. J.; McDowell, R. S.; Theaker, J. E.; Skelton, N. J. *J. Am. Chem. Soc.* **2001**, *123*, 625.
15. Santiveri, C. M.; León, E.; Rico, M.; Jiménez, M. A. *Chem. Eur. J.* **2008**, *14*, 488.
16. Bienstock, R. J.; Rizo, J.; Koerber, S. C.; Rivier, J. E.; Hagler, A. T.; Gierasch, L. M. *J. Med. Chem.* **1993**, *36*, 3265.
17. Ying, J.; Gu, X.; Cai, M.; Dedek, M.; Vagner, J.; Trivedi, D. B.; Hruby, V. J. *J. Med. Chem.* **2006**, *49*, 6888.
18. Zilberberg, L.; Shinkaruk, S.; Lequin, O.; Rousseau, B.; Hagedorn, M.; Costa, F.; Caronzolo, D.; Balke, M.; Canron, X.; Convert, O.; Laïn, G.; Gionnet, K.; Gonçalves, M.; Bayle, M.; Bello, L.; Chassaing, G.; Deleris, G.; Bikfalvi, A. *J. Biol. Chem.* **2003**, *278*, 35564.
19. Robinson, J. A. *Acc. Chem. Res.* **2008**, *41*, 1278.
20. Lombardi, A.; Dauria, G.; Saviano, M.; Maglio, O.; Nastri, F.; Quartara, L.; Pedone, C.; Pavone, V. *Biopolymers* **1996**, *40*, 505.
21. Bisang, C.; Weber, C.; Inglis, J.; Schiffer, C. A.; van Gunsteren, W. F.; Jelesarov, I.; Bosshard, H. R.; Robinson, J. A. *J. Am. Chem. Soc.* **1995**, *117*, 7904.
22. Welsh, J. H.; Zerbe, O.; von Philipsborn, W.; Robinson, J. A. *FEBS Lett.* **1992**, *297*, 216.
23. *Solid-Phase Synthesis. A Practical Guide*; Kates, S. A., Albericio, F., Eds.; Marcel-Dekker, 2000. p 143; Chapter 4.
24. Lamthanh, H.; Roumestand, C.; Deprun, C.; Ménez, A. *Int. J. Peptide Protein Res.* **1993**, *41*, 85.
25. Zamborelli, T. J.; Dodson, W. S.; Harding, B. J.; Zhang, J.; Bennett, B. D.; Lenz, D. M.; Liu, C. F.; Jones, T.; Jarosinski, M. A.; Young, Y.; Haniu, M. *J. Pept. Res.* **2000**, *55*, 359.
26. Söll, R.; Beck-Sickinger, A. G. *J. Pept. Sci.* **2000**, *6*, 387.
27. Sheridan, J. M.; Hayes, G. M.; Austen, B. M. *J. Pept. Sci.* **1999**, *5*, 555.
28. Page, K.; Hood, C. A.; Patel, H.; Fuentes, G.; Menakuru, M.; Park, J. H. *J. Pept. Sci.* **2007**, *13*, 833.
29. *Solid-Phase Synthesis. A Practical Guide*; Kates, S. A., Albericio, F., Eds.; Marcel Dekker: New York, Basel, 2000.
30. Valeur, E.; Bradley, M. *Chem. Soc. Rev.* **2009**, *38*, 606.
31. Welsh, J. H.; Zerbe, O.; von Philipsborn, W.; Robinson, J. A. *FEBS Lett.* **1992**, *297*, 216.
32. Schubert, M.; Labudde, D.; Oschkinat, H.; Schmieder, P. *J. Biomol. NMR* **2002**, *24*, 149.
33. Delaney, N. G.; Madison, V. *J. Am. Chem. Soc.* **1982**, *104*, 6635.
34. Santiveri, C.; Rico, M.; Jiménez, M. A. *J. Biomol. NMR* **2001**, *19*, 331.
35. Wishart, D. S.; Bigam, C. G.; Holm, A.; Hodges, R. S.; Sykes, B. D. *J. Biomol. NMR* **1995**, *5*, 61.
36. Cierpicki, T.; Otlewski, J. *J. Biomol. NMR* **2001**, *21*, 249.
37. Goncalves, V.; Gautier, B.; Garbay, C.; Vidal, M.; Inguimbert, N. *Anal. Biochem.* **2007**, *366*, 108.
38. Gautier, B.; Goncalves, V.; Diana, D.; Di Stasi, R.; Teillet, F.; Lenoir, C.; Huguenot, F.; Garbay, C.; Fattorusso, R.; D'Andrea, L. D.; Vidal, M.; Inguimbert, N. *J. Med. Chem.* **2010**, *53*, 4428.
39. *Fmoc Solid Phase Peptide Synthesis. A practical approach*; Chan, W. C., White, P. D., Eds.; Oxford University Press: New York, 2000.
40. Fields, G. B. *Int. J. Peptide Protein Res.* **1990**, *35*, 161.
41. *Synthetic Peptides*; Grant, G., Ed.; W. H. Freeman & Co.: New York, 1992.

42. Rink, H. *Tetrahedron Lett.* **1987**, *28*, 3787.
43. Case, D. A.; Darden, T. A.; Cheatham, I. T. E.; Simmerling, C. L.; Wang, J.; Duke, R. E.; Luo, R.; Crowley, M.; Walker, R. C.; Zhang, W.; Merz, K. M.; Wang, B.; Hayik, S.; Roitberg, A.; Seabra, G.; Kolossváry, I.; Wong, K. F.; Paesani, F.; Vanicek, J.; Wu, X.; Brozell, S. R.; Steinbrecher, T.; Gohlke, H.; Yang, L.; Tan, C.; Mongan, J.; Hornak, V.; Cui, G.; Mathews, D. H.; Seetin, M. G.; Sagui, C.; Babin, V.; Kollman, P. A. *AMBER version 10*; University of California: San Francisco, 2008.
44. Pearlman, D. A.; Case, J. W.; Caldwell, W. S.; Ross, T. E.; Cheatham, I.; DeBolt, S.; Ferguson, D.; Seibel, G.; Kollman, P. *Compd. Phys. Commun.* **1995**, *91*, 1.
45. Case, D. A.; Cheatham, T.; Darden, T.; Gohlke, H.; Luo, R.; Merz, K. M.; Onufriev, J. A.; Simmerling, C.; Wang, B.; Woods, R. *R. J. Computat. Chem.* **2005**, *26*, 1668.
46. Santiveri, C. M.; Pantoja-Uceda, D.; Rico, M.; Jimenez, M. A. *Biopolymers* **2005**, *79*, 150.
47. TOPSPIN, p. NMR Data Acquisition and Processing Software, Bruker Biospin, Karlsruhe (Germany).
48. Wishart, D. S.; Bigam, C. G.; Yao, J.; Abildgaard, F.; Dyson, H. J.; Oldfield, E.; Markley, J. L.; Sykes, B. D. *J. Biomol. NMR* **1995**, *6*, 135.
49. Wuthrich, K. *NMR of Proteins and Nucleic Acids*; John Wiley & Sons: New York, 1986.
50. Wuthrich, K.; Billeter, M.; Braun, W. *J. Mol. Biol.* **1984**, *180*, 715.